

Facile Synthesis of High Quality TiO₂ Nanocrystals in Ionic Liquid via a Microwave-Assisted Process

Kunlun Ding, Zhenjiang Miao, Zhimin Liu,* Zhaofu Zhang, Buxing Han, Guimin An, Shiding Miao, and Yun Xie

Beijing National Laboratory for Molecular Sciences (BNLMS), Center for Molecular Science, Institute of Chemistry, The Chinese Academy of Sciences, Beijing 100080, China

Received February 4, 2007; E-mail: liuzm@iccas.ac.cn

Colloidal nanocrystals (NCs) have attracted great attention because of their so-called size- and shape-dependent physical properties. The ability to control the uniformity of the size, shape, composition, crystal structure, and surface properties of the nanocrystals is essential for uncovering their intrinsic properties unaffected by sample heterogeneity. Controlled growth of monodisperse nanocrystals is critical for studying and exploiting their unique properties.¹ TiO₂ is one of the most studied NCs owing to its wide applications, such as pigments, photocatalysts, catalyst supports, solar-cell, gas sensors, and so on.² Although many efforts have been made on controlling TiO₂ crystal structure, size, and shapes via wet chemistry,² it is still a challenge to synthesize high quality TiO₂ NCs on a large scale.

Ionic liquids (ILs) have been widely studied as a new kind of reaction media owing to their unique properties such as extremely low volatility, wide liquid temperature range, good thermal stability, good dissolving ability, excellent microwave (MW) absorbing ability, designable structures, high ionic conductivity, and wide electrochemical window, etc.^{3a} In recent years, many inorganic nanostructures have been fabricated via various IL-involved processes, including electrodeposition, chemoreduction, sol-gel and solvothermal route.^{3b-f} While there still exist some problems, ILs have already been proved to be excellent media for inorganic synthesis.

Herein we report a facile method to synthesize anatase NCs with uniform size and shape via a microwave-assisted route in IL. This method has some obvious advantages: the process is fast and simple; the reaction can be performed under atmospheric pressure in a domestic microwave oven; no high-pressure and high-temperature apparatus is needed; the size of NCs can be easily controlled. The NCs are highly crystalline, low in Ti³⁺ defect, and free of aggregation. We believe that this method can be developed into a general way to synthesize metal oxide NCs.

We used IL, 1-butyl-3-methylimidazolium tetrafluoroborate ([bmim]⁺[BF₄]⁻), as solvent and titanium isopropoxide (TTIP) as precursor for the synthesis of TiO₂ NCs, and experimental details are given in Supporting Information. Transmission electron microscopy (TEM) images of the NCs are shown in Figure 1. Most of NCs displayed cubelike shape under low-magnification TEM observation (Figure 1a), while two kinds of 2D lattice fringes were observed (Figure 1 panels b and c) via detailed high-resolution TEM (HRTEM) tilted angle analysis, which agreed with the truncated bipyramid shape (Figure 1d). The HRTEM images in Figure 1b, c, respectively, fit well with simulated HRTEM images (Figure 1e, f) viewed along a- and b-directions marked in Figure 1d. Therefore, we suppose the NCs exhibited bipyramid shape with highly truncated (001) facets, and thus most of them stood on copper grid parallel to [001] direction and showed cubelike shape under low-magnification TEM observation.

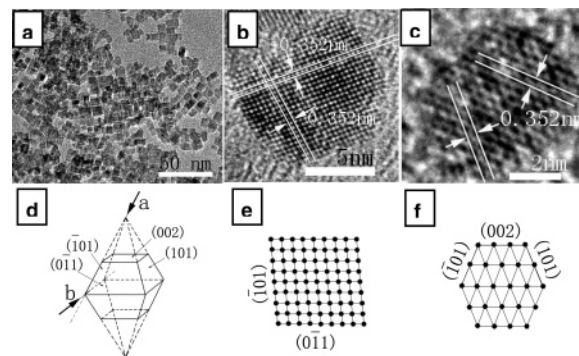


Figure 1. (a) TEM image, (b and c) HRTEM images of the sample prepared via microwave irradiation for 40 min, (d) simulated shape of NCs, (e and f) simulated HRTEM images of (d) along a- and b-direction, respectively.

The XRD pattern of the sample (Figure S1, Supporting Information) matched well with the standard pattern of anatase (JCPDS 21-1272); moreover, there is no observable diffraction peaks at 27° or 31°, indicating that the NCs were free of rutile and brookite impurities. The average size calculated from the most intense diffraction peak (101) using the Debye-Scherrer equation⁴ was 9 nm, which was similar to TEM observation (Figure 1a). X-ray photoelectron spectroscopy analysis gave further information about the NCs. All Ti 2p signals (Figure S2) were highly symmetric, and no shoulders were observed at the lower energy sides of the strong Ti 2p signals, suggesting the defect concentration associated with Ti³⁺ was extremely low.^{2d} The UV-vis absorption and photoluminescence (PL, room temperature, excited at 250 nm) emission behaviors of the NCs in ethanol are shown in Figure S3. The UV-vis absorption spectrum was typical for anatase.^{2c,f} The PL spectrum exhibited two main peaks. The band centered around 398 nm could be assigned to band-to-band transitions,⁵ and the other at 468 nm was related to surface trap state owing to incomplete surface passivation, where radiationless recombination occurred. Additionally, no peak was observed between 600 and 800 nm, which was associated with the transition of electrons from the conduction band edge to holes, trapped at an interstitial Ti³⁺ site.⁵ This further suggests that there was negligible Ti³⁺ defect in the NCs, which agreed well with XPS analysis. The crystal size of the NCs could be tuned by changing reaction time and water content in IL. Both increases in reaction time and water content resulted in NCs with larger size (Figure S4).

To investigate the formation mechanism of TiO₂ NCs, we characterized some intermediates by FTIR, Raman, and HRTEM observation. As described in experimental procedures (see Supporting Information), the reaction system became clear after evaporating ethanol from IL solution, suggesting a soluble Ti-complex (denoted as sample A) was formed in IL, which might play a key role in the formation of the final product. Sample A

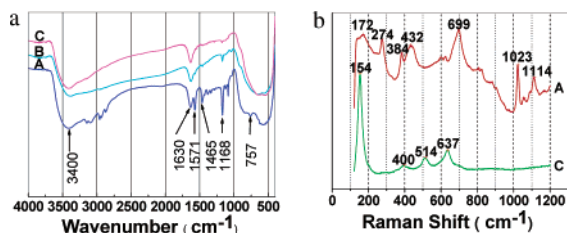


Figure 2. FTIR (a) and Raman (b) spectra of the products obtained at different microwave radiation times after evaporating ethanol: A, 0 min; B, 3 min; C, 40 min.

was separated from the solution via precipitation by dichloromethane and washed with dichloromethane for several times. In the FTIR spectrum of sample A (Figure 2a), the absorption bands at 757, 1168, 1465, and 1571 cm^{-1} belong to $[\text{bmim}]^+$,^{6a,b} indicating that sample A contained $[\text{bmim}]^+$ species. However, the absorption at 1168 cm^{-1} was different from that in bulk $[\text{bmim}]^+[\text{BF}_4]^-$, suggesting that the chemical environment of these $[\text{bmim}]^+$ species was different from that in bulk $[\text{bmim}]^+[\text{BF}_4]^-$. The band centered around 3400 cm^{-1} ascribes to the hydroxyl group of Ti–O–H, and the weak absorption centered around 1630 cm^{-1} is associated with the deformation vibration of H–O–H bonds from the physisorbed water.^{2d} Figure 2b shows Raman spectra of sample A and the final product. Considering no strong band located in the range of 900–1200 cm^{-1} on Raman spectrum of $[\text{bmim}]^+[\text{BF}_4]^-$, the bands at 1023 cm^{-1} and 1114 cm^{-1} in the spectrum of sample A should be assigned to Ti–O–R, and bands at 172, 274, 384, 432, and 699 cm^{-1} are similar to those of titanate.^{6c,d} FTIR and Raman analysis indicate that sample A was possibly IL-stabilized polyanions, originated from TTIP hydrolysis and condensation at an early stage of the process.

The solid intermediate obtained via microwave irradiation for 3 min (denoted as sample B) was examined by HRTEM observation. As shown in Figure S5, lamellar structures were formed in sample B, whose interlayer distance was 1.1 nm, larger than those of $\text{H}_2\text{-Ti}_3\text{O}_7$ (0.78 nm) and $\text{Na}_2\text{Ti}_3\text{O}_7$ (0.84 nm).⁷ This implies that $[\text{bmim}]^+$ might be present in the interlayer. It was confirmed by FTIR result (Figure 2a, band at 1168 cm^{-1} on spectrum B assigned to $[\text{bmim}]^+$). HRTEM image of sample B (Figure S5b) displays two kinds of structures: region A attributed to titanate and region B attributed to anatase. The coexistence of titanate and anatase in the same domain indicates transformation from titanate to anatase. For the final product obtained via microwave irradiation for 40 min (denoted as sample C), FTIR spectrum (spectrum C in Figure 2a) showed a very weak absorption at 1168 cm^{-1} , indicating the presence of trace $[\text{bmim}]^+$ at the surface of TiO_2 NCs; while Raman spectrum (spectrum C in Figure 2b) matched well with standard Raman spectrum of anatase.

On the basis of the partial charge model theory^{2b,8} and our experimental results, we proposed a possible formation mechanism of TiO_2 NCs. At the early stage of the reaction process, TTIP was hydrolyzed by a small amount of water in the IL and then condensed into short-chain polyanions (i.e., oligomer). These polyanions were protected by $[\text{bmim}]^+$ cations and dissolved in the IL to form homogeneous solution. Since the temperature rose rapidly after removal of ethanol from IL solution because of the strong microwave absorption ability of IL, fast growth and cross-linking of these polyanions occurred, achieving the nucleation burst. Followed by the rapid growth of these nuclei, anatase NCs were

formed within several minutes. In this method, IL played multiple roles: it not only served as a reaction medium, but also as a microwave absorbent; furthermore, it acted as a protecting agent for intermediates and anatase NCs. Considering that anatase has a tetragonal structure and tends to nucleate as truncated octagonal bipyramid seeds,⁹ the fact that the NCs prepared in this work possessed truncated bipyramid shape indicates that less selective crystal growth occurred. This may be due to the weak ligand protection of $[\text{bmim}]^+$ for the NCs. Actually, few dendritic NCs were observed in sample C (Figure S6), which probably resulted from oriented-attachment of truncated bipyramid-shaped NCs, indicating that $[\text{bmim}]^+$ can only provide weak protection for anatase NCs. To further confirm this, oleic acid (that is known to bind strongly to certain surfaces of anatase)^{2a,g} was used as an additive to this system, which resulted in some 1-D structures similar to those reported in literature^{2a,g} (Figure S7).

The above method also can be extended to the synthesis of some other metal oxide NCs. For example, SnO_2 NCs were successfully synthesized via similar procedures (Figures S8 and S9).

In conclusion, we have demonstrated a facile way to synthesize size-controlled anatase NCs. These NCs may be useful for basic studies on size- and shape-dependent properties of TiO_2 . We believe that this method will open a new way to fabricate nanostructure materials, and systematic study is in progress.

Acknowledgment. This work is financially supported by National Natural Science Foundation of China (Grant No. 20533010).

Supporting Information Available: Experimental procedures, XRD patterns, XPS spectra, UV–vis and FL spectra, TEM images (Figures S1–S7) of TiO_2 NCs, TEM image and XRD pattern of SnO_2 NCs (Figures S8–S9). This material is available free of charge via the Internet at <http://pubs.acs.org>.

References

- (1) (a) Yin, Y. D.; Alivisatos, A. P. *Nature* **2005**, *437*, 664. (b) Peng, X. G.; Thessing, J. *Struct. Bonding (Berlin)* **2005**, *118*, 79.
- (2) (a) Cozzoli, P. D.; Kornowski, A.; Weller, H. *J. Am. Chem. Soc.* **2003**, *125*, 14539. (b) Chemseddine, A.; Moritz, T. *Eur. J. Inorg. Chem.* **1999**, *1999*, 235. (c) Zhang, H. Z.; Finnegan, M.; Banfield, J. F. *Nano Lett.* **2001**, *1*, 81. (d) Li, G. S.; Li, L. P.; Boerio-Goates, J.; Woodfield, B. F. *J. Am. Chem. Soc.* **2005**, *127*, 8659. (e) Zhu, H. Y.; Lan, Y.; Gao, X. P.; Ringer, S. P.; Zheng, Z. F.; Song, D. Y.; Zhao, J. C. *J. Am. Chem. Soc.* **2005**, *127*, 6730. (f) Mao, Y. B.; Wong, S. S. *J. Am. Chem. Soc.* **2006**, *128*, 8217. (g) Jun, Y.; Casula, M. F.; Sim, J.; Kim, S. Y.; Cheon, J.; Alivisatos, A. P. *J. Am. Chem. Soc.* **2003**, *125*, 15981.
- (3) (a) Antonietti, M.; Kuang, D. B.; Smarsly, B.; Zhou, Y. *Angew. Chem., Int. Ed.* **2004**, *43*, 4988. (b) Endres, F. *ChemPhysChem* **2002**, *3*, 144. (c) Dupont, J.; Fonseca, G. S.; Umpierre, A. P.; Fichtner, P. F. P.; Teixeira, S. R. *J. Am. Chem. Soc.* **2002**, *124*, 4228. (d) Zhou, Y.; Antonietti, M. *Adv. Mater.* **2003**, *15*, 1452. (e) Cooper, E. R.; Andrews, C. D.; Wheatley, P. S.; Webb, P. B.; Wormald, P.; Morris, R. E. *Nature* **2004**, *430*, 1012. (f) Zhu, Y. J.; Wang, W. W.; Qi, R. J.; Hu, X. L. *Angew. Chem., Int. Ed.* **2004**, *43*, 1410.
- (4) Klug, H. P.; Alexander, L. E. *X-ray Diffraction Procedures*; John Wiley & Sons: New York, **1959**.
- (5) (a) Pan, D. C.; Zhao, N. N.; Wang, Q.; Jiang, S. C.; Ji, X. L.; An, L. J. *Adv. Mater.* **2005**, *17*, 1991. (b) Liu, Y. J.; Claus, R. O. *J. Am. Chem. Soc.* **1997**, *119*, 5273.
- (6) (a) Koel, M. *Proc. Estonian Acad. Sci. Chem.* **2000**, *49*, 145. (b) Talaty, E. R.; Raja, S.; Storhaug, V. J.; Dölle, A.; Carper, W. R. *J. Phys. Chem. B* **2004**, *108*, 13177. (c) Urlaub, R.; Posset, U.; Thull, R. *J. Non-Cryst. Solids* **2000**, *265*, 276. (d) Kolen'ko, Y. V.; Kovnir, K. A.; Gavrilov, A. I.; Garshev, A. V.; Frantti, J.; Lebedev, O. I.; Churagulov, B. R.; Tendeloo, G. V.; Yoshimura, M. *J. Phys. Chem. B* **2006**, *110*, 4030.
- (7) Chen, Q.; Zhou, W. Z.; Du, G. H.; Peng, L. M. *Adv. Mater.* **2002**, *14*, 1208.
- (8) Henry, M.; Jolivet, J. P.; Livage, J. *Struct. Bonding (Berlin)* **1992**, *77*, 155.
- (9) Penn, R. L.; Banfield, J. F. *Geochim. Cosmochim. Acta* **1999**, *63*, 1549.

JA070809C